Journal of Zhejiang University SCIENCE A
ISSN 1009-3095 (Print); ISSN 1862-1775 (Online)
www.zju.edu.cn/jzus; www.springerlink.com
E-mail: jzus@zju.edu.cn

Finite element analysis of dynamic stability of skeletal structures under periodic loading

THANA Hemantha Kumar, AMEEN Mohammed
(*Department of Civil Engineering, National Institute of Technology, Calicut, Kerala 673601, India*)
E-mail: hemanth0252000@yahoo.co.in; ameen@nitc.ac.in
Received Apr. 23, 2006; revision accepted Oct. 21, 2006

Abstract: This paper addresses the dynamic stability problem of columns and frames subjected to axially applied periodic loads. Such a structure can become unstable under certain combinations of amplitudes and frequencies of the imposed load acting on its columns/beams. These are usually shown in the form of plots which describe regions of instability. The finite element method (FEM) is used in this work to analyse dynamic stability problems of columns. Two-noded beam elements are used for this purpose. The periodic loading is decomposed into various harmonics using Fourier series expansion. Computer codes in C++ using object oriented concepts are developed to determine the stability regions of columns subjected to periodic loading. A number of numerical examples are presented to illustrate the working of the program. The direct integration of the equations of motions of the discretised system is carried out using Newmark's method to verify the results.

Key words: Finite element analysis, Dynamic stability, Mathieu-Hill equation
doi:10.1631/jzus.2007.A0245 **Document code:** A **CLC number:** U448.25

INTRODUCTION

Some structures fail geometrically before the strength failure because of lack of stability and such a failure is known as instability failure or buckling failure. Determination of buckling load is important in order to ensure the stability of a structure. If the structure under consideration is subjected to a dynamic load then this problem comes under the purview of dynamic stability problems. Examples are slender offshore structures subjected to periodic excitations and columns in the lower floor of a building subjected to periodic excitation due to machinery on the higher floors.

Bolotin (1964) addressed the dynamic stability problem of mechanical systems as early as 1964. Several works have been reported thereafter along the lines. These works tend to quantify the instability phenomenon of slender structures under the action of time-varying harmonic loads. The governing differential equation of a beam-column subjected to axially applied harmonic forces boil down to Mathieu-Hill equations (Bolotin, 1964; McLachlan, 1957; Zounes and Rand, 1998). The closed-form solution of this equation is difficult for slender columns and frames with different configurations and support conditions.

Briseghella *et al*.(1998) demonstrated the use of finite element method (FEM) in dynamic stability problems of beams and frames. They, however, considered only harmonic loads. Park and Jung (2002) presented numerical analysis of lateral response of a long slender marine structure under combined parametric and forcing excitations using FEM in the time domain using the Newmark constant acceleration method. Sugiyama *et al*.(2000) carried out experimental verification of the effect of non-conservative follower force on the vibration and stability of cantilevered columns. Solid rocket motors where used to give a sudden thrust which acted tangential to the column tip. Sygulski (1996) studied the aeroelastic dynamic stability of 3D pneumatic structures in wind flow. Both computational and experimental investigations were carried out. The dynamic stability problems of cracked cylindrical shells were addressed

by Javidruzi *et al*.(2004).

The present paper addresses the use of FEM in solving dynamic stability problems of slender columns and frames subjected to axially applied periodic loads. Two-noded Euler beam elements are used for modelling the structure. At each node the transverse displacement and rotation degrees of freedom are considered. By applying the total energy principle, the system of Mathieu-Hill differential equation is arrived at. The regions of instability are determined by substituting the periodic solution in Mathieu-Hill differential equation. The solution is carried out for undamped and damped cases by using the Jacobi's method (as an algebraic eigenvalue problem) and the secant method respectively. A number of numerical examples are presented to illustrate the effectiveness of the proposed method. For each of the problems, the direct integration method is used to check the correctness of the instability regions found. The proposed method can be used for analysing columns and skeletal frames although numerical examples consider only slender columns.

GOVERNING DIFFERENTIAL EQUATIONS

The continuum model presented by Bolotin (1964) for a slender column subjected to harmonic or periodic loading as depicted in Fig.1 can be systematically extended using the finite element concepts to arrive at a system of Mathieu-Hill differential equations (McLachlan, 1957), the number of equations depending on the number of degrees of freedom which in turn depends on the finite element discretisation.

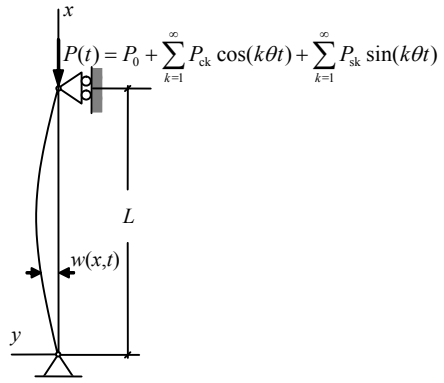

Fig.1 Column subjected to a periodic load

The slender column or frame is discretised by using two-noded Euler beam elements with two degrees of freedom at each node as depicted in Fig.2. The transverse displacement $w(x)$ of the element is interpolated from the nodal degrees of freedom using the standard cubic hermitian interpolation polynomials (Cook *et al*., 2003):

$$N_1=1-3x^2/l^2+2x^3/l^3,\ \ N_2=x-2x^2/l+x^3/l^2,$$
$$N_3=3x^2/l^2-2x^3/l^3,\ \ N_4=-x^2/l+x^3/l^2,$$

and can be written as

$$w(x)=[N_1\quad N_2\quad N_3\quad N_4]\begin{Bmatrix}q_1\\q_2\\q_3\\q_4\end{Bmatrix}=[\boldsymbol{N}]\{\boldsymbol{q}\}. \tag{1}$$

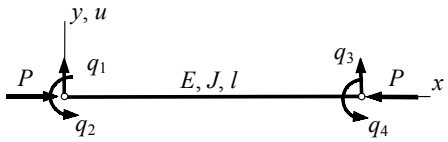

Fig.2 Two-noded beam element

E is the modulus of elasticity, J is the second moment of area of the beam cross-section, and l is the length of the element

The generalised strain κ (viz., the curvature) is given by

$$\kappa(x)=\frac{\mathrm{d}^2w}{\mathrm{d}x^2}=\frac{\mathrm{d}^2}{\mathrm{d}x^2}[\boldsymbol{N}]\boldsymbol{q}=[\boldsymbol{B}]\boldsymbol{q}, \tag{2}$$

and the generalised stress $M(x)$ (viz., the bending moment) is given by

$$M(x)=EI\frac{\mathrm{d}^2w}{\mathrm{d}x^2}=EI[\boldsymbol{B}]\boldsymbol{q}. \tag{3}$$

The total energy principle can be used to obtain the equations of motion. According to this principle, the total energy (E_t) stored in a conservative system is a constant and therefore its rate of change with respect to time is zero. That is

$$\frac{\mathrm{d}E_t}{\mathrm{d}t}=0. \tag{4}$$

The total energy stored in the system is equal to

the sum of kinetic energy and potential energy. Making use of Eqs.(1) to (3), Eq.(4) can be written as

$$\frac{\mathrm{d}E_{\mathrm{t}}}{\mathrm{d}t}=\frac{\mathrm{d}}{\mathrm{d}t}\left\{\frac{1}{2}\left(\int_0^l EI\,\kappa^2\mathrm{d}x-\int_0^l P(t)w'^2\mathrm{d}x+\int_0^l m\dot{w}^2\mathrm{d}x\right)\right\}=0,$$

where $P(t)$ is the axially applied dynamic load and m is the mass per unit length of the beam; the first term on the right hand side within the parantheses represents the strain energy, the second the potential of the axially applied load and the last term the kinetic energy. This equation can be simplified using Eqs.(1)~(3) to obtain

$$([\boldsymbol{k}]-P(t)[\boldsymbol{s}])\{\boldsymbol{q}\}+[\boldsymbol{m}]\{\ddot{\boldsymbol{q}}\}=\{\boldsymbol{0}\}, \tag{5}$$

where $[\boldsymbol{k}]$, $[\boldsymbol{m}]$ and $[\boldsymbol{s}]$ are the element stiffness, mass and stability (or geometric stiffness) matrices respectively, $P(t)$ is the periodic load acting axially, and $\{\boldsymbol{q}(t)\}$ is the vector degree of freedom. These matrices are given by (Cook *et al*., 2003):

$$[\boldsymbol{k}]=\int_0^l[\boldsymbol{B}]^{\mathrm{T}}[\boldsymbol{D}][\boldsymbol{B}]\mathrm{d}x=\frac{EI}{l^3}\begin{bmatrix}12 & 6l & -12 & 6l\\ 6l & 4l^2 & -6l & 2l^2\\ -12 & -6l & 12 & -6l\\ 6l & 2l^2 & -6l & 4l^2\end{bmatrix},$$

$$[\boldsymbol{m}]=\int_0^l[\boldsymbol{N}]^{\mathrm{T}}m[\boldsymbol{N}]\mathrm{d}x=\frac{m}{420}\begin{bmatrix}156 & 22l & 54 & -13l\\ 22l & 4l^2 & 13l & -3l^2\\ 54 & 13l & 156 & -22l\\ -13l & -3l^2 & -22l & 4l^2\end{bmatrix},$$

$$[\boldsymbol{s}]=\int_0^l[\boldsymbol{N}']^{\mathrm{T}}[\boldsymbol{N}']\mathrm{d}x=\frac{1}{30l}\begin{bmatrix}36 & 3l & -36 & 3l\\ 3l & 4l^2 & -3l & -l^2\\ -36 & -3l & 36 & -3l\\ 3l & -l^2 & -3l & 4l^2\end{bmatrix}.$$

The given skeletal structure is discretised into beam elements. The element matrices as noted above are assembled to obtain the global equations of motion. The assembled equations including the effects of damping can be written as

$$\boldsymbol{M}\ddot{\boldsymbol{q}}+\boldsymbol{C}\dot{\boldsymbol{q}}+\{\boldsymbol{K}-P(t)\boldsymbol{S}\}\boldsymbol{q}=\boldsymbol{0}, \tag{6}$$

where $\boldsymbol{M}$, $\boldsymbol{C}$, $\boldsymbol{K}$ and $\boldsymbol{S}$ are the global mass, damping, stiffness and stability matrices, respectively. Care needs to be exercised while assembling the matrices to ensure that the stability matrix $[\boldsymbol{s}]$ is included only for those elements across which the dynamic axial load acts. This is especially important in the case of frames where the axial load may occur only across columns. Eq.(6) is the system of Mathieu-Hill differential equations and represents the equations of motion of the system including the effects of damping.

The periodic load $P(t)$ can be represented using the Fourier series as

$$P(t)=P_0+\sum_{k=1}^{\infty}P_{ck}\cos(k\theta t)+\sum_{k=1}^{\infty}P_{sk}\sin(k\theta t), \tag{7}$$

where the coefficients are given by

$$P_0=\frac{1}{T}\int_0^T P(t)\mathrm{d}t,\quad P_{ck}=\frac{2}{T}\int_0^T P(t)\cos(k\theta t)\mathrm{d}t,$$

$$P_{sk}=\frac{2}{T}\int_0^T P(t)\sin(k\theta t)\mathrm{d}t,\qquad k=0,\,1,\,2,\,\ldots$$

Denoting the period of $P(t)$ by T, we have $P(t+T)=P(t)$.

The damping matrix of Eq.(6) may be taken to be proportional to the mass and stiffness matrices in the usual way (Cook *et al*., 2003; Bathe, 1998) as

$$\boldsymbol{C}=\alpha\boldsymbol{M}+\beta\boldsymbol{K},$$

where α and β are constants. Substituting this in Eq.(6) and premultiplying by $\boldsymbol{K}^{-1}$, we obtain

$$\boldsymbol{K}^{-1}\boldsymbol{M}\ddot{\boldsymbol{q}}+(\alpha\boldsymbol{K}^{-1}\boldsymbol{M}+\beta\boldsymbol{I})\dot{\boldsymbol{q}}+\{\boldsymbol{I}-P(t)\,\boldsymbol{K}^{-1}\boldsymbol{S}\}\boldsymbol{q}=\boldsymbol{0}. \tag{8}$$

Eq.(8) is a system of coupled second order homogeneous linear differential equations. One may assume a suitable solution and substitute this into Eq.(8). Generally when we consider damping, we expect the solution to be decaying with time. That is, the displacement should gradually decrease with time. Hence, we may assume the displacement vector in the form

$$\boldsymbol{q}(t)=\boldsymbol{u}(t)\,\mathrm{e}^{-\xi t},$$

where the presence of $\mathrm{e}^{-\xi t}$ indicates that the

displacement dies out with time. Substituting this solution in Eq.(8) yields

$$\boldsymbol{K}^{-1}\boldsymbol{M}\ddot{\boldsymbol{u}}+(-2\xi\boldsymbol{K}^{-1}\boldsymbol{M}+\alpha\boldsymbol{K}^{-1}\boldsymbol{M}+\beta\boldsymbol{I})\dot{\boldsymbol{u}}+\{\xi^2\boldsymbol{K}^{-1}\boldsymbol{M}-\xi(\alpha\boldsymbol{K}^{-1}\boldsymbol{M}+\beta\boldsymbol{I})+[\boldsymbol{I}-P(t)\boldsymbol{K}^{-1}\boldsymbol{S}]\}\boldsymbol{u}=\boldsymbol{0}.$$

The term involving $\dot{\boldsymbol{u}}$ can be dispensed with altogether by choosing the proportional damping coefficients as $\alpha=2\xi$ and $\beta=0$. Then we get

$$\boldsymbol{K}^{-1}\boldsymbol{M}\ddot{\boldsymbol{u}}+\{\boldsymbol{I}-\xi^2\boldsymbol{K}^{-1}\boldsymbol{M}-P(t)\boldsymbol{K}^{-1}\boldsymbol{S}\}\boldsymbol{u}=\boldsymbol{0}.$$

The above equation can be rewritten as

$$\frac{\mathrm{d}^2\boldsymbol{u}}{\mathrm{d}t^2}+\boldsymbol{\Phi}(t)\boldsymbol{u}=\boldsymbol{0}, \tag{9}$$

where

$$\boldsymbol{\Phi}(t)=\boldsymbol{M}^{-1}[\boldsymbol{K}-\xi^2\boldsymbol{M}-P(t)\boldsymbol{S}]. \tag{10}$$

The system of n coupled second order differential equations represented by Eq.(9) could be transformed into an equivalent system of $2n$ first order differential equations by making use of the substitutions

$$x_i=u_i \text{ and } x_{n+i}=\mathrm{d}u_i/\mathrm{d}t,\ i=1, 2, \ldots, n,$$

to obtain

$$\frac{\mathrm{d}\boldsymbol{x}}{\mathrm{d}t}+\boldsymbol{\Phi}'(t)\boldsymbol{x}(t)=\boldsymbol{0}, \tag{11}$$

where

$$\boldsymbol{\Phi}'(t)_{2n\times 2n}=\begin{bmatrix}\boldsymbol{0} & -\boldsymbol{I}\\ \boldsymbol{\Phi} & \boldsymbol{0}\end{bmatrix}.$$

Denoting the $2n\times 2n$ solution matrix obtained after substituting the $2n$ linearly independent solutions of Eq.(11) by $\boldsymbol{X}(t)$, we can write (Meirovitch, 1970)

$$\frac{\mathrm{d}\boldsymbol{X}}{\mathrm{d}t}+\boldsymbol{\Phi}'(t)\boldsymbol{X}(t)=\boldsymbol{0}. \tag{12}$$

The periodicity of the solutions can be used to advantage while solving the above system of homogeneous linear first order differential equations. If $\boldsymbol{X}(t)$ is a solution of Eq.(12), $\boldsymbol{X}(t+T)$ must also be a solution. As a result, it is possible to write

$$\boldsymbol{X}(t+T)=\boldsymbol{R}\,\boldsymbol{X}(t), \tag{13}$$

where $\boldsymbol{R}$ acts as a transformation matrix. Bringing in an additional transformation to Eq.(13) by using another transformation matrix $\boldsymbol{P}$ defined as

$$\boldsymbol{X}(t)=\boldsymbol{P}\,\boldsymbol{Y}(t), \tag{14}$$

we can write Eq.(13) as

$$\boldsymbol{Y}(t+T)=\boldsymbol{P}^{-1}\boldsymbol{R}\,\boldsymbol{P}\,\boldsymbol{Y}(t). \tag{15}$$

We may choose the transformation matrix $\boldsymbol{P}$ such that $\boldsymbol{P}^{-1}\boldsymbol{R}\boldsymbol{P}$ is a diagonal matrix. Let us denote this diagonal matrix by $\boldsymbol{\rho}$. Therefore the above solution becomes

$$\boldsymbol{Y}(t+T)=\boldsymbol{\rho}\,\boldsymbol{Y}(t), \tag{16}$$

where $\boldsymbol{\rho}$ contains the eigenvalues of $\boldsymbol{R}$ as its diagonal elements. Eq.(16) is thus uncoupled, and therefore the kth solution can be written as

$$Y_k(t+T)=\rho_k\,Y_k(t). \tag{17}$$

Eq.(17) shows the main characteristic of the Mathieu-Hill differential equation. According to (Bolotin, 1964), depending on the value of the diagonal element ρ_k we will have stable, periodic or unstable solutions which can be summarised as

$$\begin{cases}\rho_k>1, & \text{unbounded solution;}\\ \rho_k=1, & \text{periodic solution;}\\ \rho_k<1, & \text{bounded solution.}\end{cases}$$

DETERMINATION OF INSTABILITY REGIONS

In the last section we saw how the dynamic stability problem leads to a system of uncoupled Mathieu-Hill differential equations and how its stability characteristics can be determined. The periodic solution which corresponds to $|\rho_k|=1$ characterises the boundary between the dynamic stability and instability zones. Thus, the problem of finding the regions of instability of Eq.(9) reduces to the determination of

the conditions under which it has periodic solutions.

The condition $|\rho_k|=1$ means either $\rho_k=1$ or $\rho_k=-1$. In the former case, as seen from Eq.(17), the solution of the differential equation will be periodic with a period T. On the other hand, in the latter case, the solution will have a period $2T$ as $Y_k(t+T)=-\rho_k Y_k(t)$. These are depicted in Fig.3.

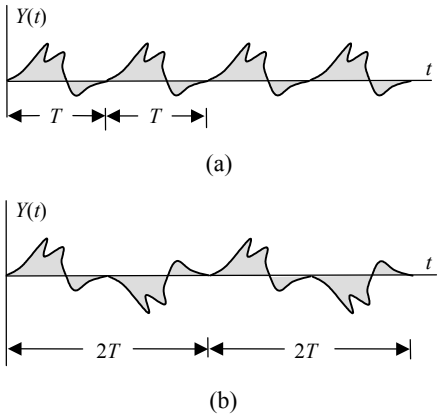

Fig.3 Solutions with period T (a) and $2T$ (b)

Consequently, the regions of unboundedly increasing solutions are separated from regions of stability by periodic solutions with periods T and $2T$. Thus, the problem of finding the regions of instability for Eq.(17) is reduced to the determination of the conditions under which it has periodic solutions with periods T and $2T$.

The conditions for the existence of periodic solutions can be obtained in an alternative way by seeking a periodic solution directly to Eq.(6). Let us seek a periodic solution with period $2T$ (where $T=2\pi/\theta$) in the form

$$q(t)=\sum_{k=1,3,5,\ldots}^{\infty}\left(a_k\sin(k\theta t/2)+b_k\cos(k\theta t/2)\right). \quad (18)$$

Substituting the series solution represented by Eq.(18) into Eq.(6) and equating the coefficients of $\sin(k\theta t/2)$ and $\cos(k\theta t/2)$ terms yield a system of linear homogeneous algebraic equations in the coefficients a_k and b_k which can be written in the following pattern:

sine coefficients at $(2n+1)$th region (at $k=2n+1$),
…,
sine coefficients at third region (at $k=3$),
sine coefficients at first region (at $k=1$),
cosine coefficients at first region (at $k=1$),
cosine coefficients at third region (at $k=3$),
…,
cosine coefficients at $(2n+1)$th region (at $k=2n+1$),
which can be written in matrix form as

$$\begin{bmatrix} \cdots & \cdots & \cdots & \cdots & \cdots & \cdots \\ \cdots & e_{11} & e_{12} & e_{13} & e_{14} & \cdots \\ \cdots & e_{21} & e_{22} & e_{23} & e_{24} & \cdots \\ \cdots & e_{31} & e_{32} & e_{33} & e_{34} & \cdots \\ \cdots & e_{41} & e_{42} & e_{43} & e_{44} & \cdots \\ \cdots & \cdots & \cdots & \cdots & \cdots & \cdots \end{bmatrix}\begin{Bmatrix} \cdots \\ a_3 \\ a_1 \\ b_1 \\ b_3 \\ \cdots \end{Bmatrix}=\mathbf{0}, \quad (19)$$

It may be noted that the assumed periodic solution with period $2T$ in Eq.(19) gives rise to only odd number of regions. For the first region, we need to consider both sine and cosine coefficients with $k=1$ only. For the third region we have to consider both sine and cosine coefficients with $k=1$ and $k=3$. Likewise we have to consider for higher regions also.

Eq.(19) is a system of homogeneous linear algebraic equations. The trivial solution (i.e. $a_1=b_1=a_3=b_3=\ldots=0$) is always a possible solution. However, nontrivial solutions are of interest. The condition for existence of nontrivial solutions is that the determinant of the coefficient matrix be equal to zero. This leads to

$$\begin{vmatrix} \cdots & \cdots & \cdots & \cdots & \cdots & \cdots \\ \cdots & \boldsymbol{I}-\frac{9\theta^2}{4}\boldsymbol{K}^{-1}\boldsymbol{M}-\left(P_0-\frac{P_{c3}}{2}\right)\boldsymbol{K}^{-1}\boldsymbol{S} & \mathbf{0} & \mathbf{0} & -3\xi\theta\boldsymbol{K}^{-1}\boldsymbol{M}-\frac{P_{s3}}{2}\boldsymbol{K}^{-1}\boldsymbol{S} & \cdots \\ \cdots & -\frac{P_{c3}}{2}\boldsymbol{K}^{-1}\boldsymbol{S} & \boldsymbol{I}-\frac{\theta^2}{4}\boldsymbol{K}^{-1}\boldsymbol{M}-\left(P_0-\frac{P_{c1}}{2}\right)\boldsymbol{K}^{-1}\boldsymbol{S} & -\xi\theta\boldsymbol{K}^{-1}\boldsymbol{M}-\frac{P_{s1}}{2}\boldsymbol{K}^{-1}\boldsymbol{S} & -\frac{P_{s3}}{2}\boldsymbol{K}^{-1}\boldsymbol{S} & \cdots \\ \cdots & -\frac{P_{s3}}{2}\boldsymbol{K}^{-1}\boldsymbol{S} & \xi\theta\boldsymbol{K}^{-1}\boldsymbol{M}-\frac{P_{s1}}{2}\boldsymbol{K}^{-1}\boldsymbol{S} & \boldsymbol{I}-\frac{\theta^2}{4}\boldsymbol{K}^{-1}\boldsymbol{M}-\left(P_0+\frac{P_{c1}}{2}\right)\boldsymbol{K}^{-1}\boldsymbol{S} & -\frac{P_{c3}}{2}\boldsymbol{K}^{-1}\boldsymbol{S} & \cdots \\ \cdots & -3\xi\theta\boldsymbol{K}^{-1}\boldsymbol{M}-\frac{P_{s3}}{2}\boldsymbol{K}^{-1}\boldsymbol{S} & \mathbf{0} & \mathbf{0} & \boldsymbol{I}-\frac{9\theta^2}{4}\boldsymbol{K}^{-1}\boldsymbol{M}-\left(P_0+\frac{P_{c3}}{2}\right)\boldsymbol{K}^{-1}\boldsymbol{S} & \cdots \\ \cdots & \cdots & \cdots & \cdots & \cdots & \cdots \end{vmatrix}=\mathbf{0}. \quad (20)$$

Let us first consider the first region alone which is retained from Eq.(20) and shown below as

$$\begin{vmatrix} \boldsymbol{I}-\frac{\theta^2}{4}\boldsymbol{K}^{-1}\boldsymbol{M}-\left(P_0+\frac{P_{c1}}{2}\right)\boldsymbol{K}^{-1}\boldsymbol{S} & -\xi\theta\boldsymbol{K}^{-1}\boldsymbol{M}-\frac{P_{s1}}{2}\boldsymbol{K}^{-1}\boldsymbol{S} \\ \xi\theta\boldsymbol{K}^{-1}\boldsymbol{M}-\frac{P_{s1}}{2}\boldsymbol{K}^{-1}\boldsymbol{S} & \boldsymbol{I}-\frac{\theta^2}{4}\boldsymbol{K}^{-1}\boldsymbol{M}-\left(P_0+\frac{P_{c1}}{2}\right)\boldsymbol{K}^{-1}\boldsymbol{S} \end{vmatrix}=\boldsymbol{0}. \tag{21}$$

Eq.(21) makes it possible to calculate the boundaries of the regions of instability. In determining the first region, the basic unknown is the loading frequency θ with all the remaining being known parameters. So by equating the determinant of the first region matrix to zero, we can find the value of θ. In this work an important task is to find the θ values by equating the determinant of the above matrix to zero. We consider the undamped and damped cases separately.

Undamped case

In this case, the proportional damping factor ξ is zero. Therefore the determinant of the first region matrix reduces to

$$\begin{vmatrix} \boldsymbol{I}-\frac{\theta^2}{4}\boldsymbol{K}^{-1}\boldsymbol{M}-\left(P_0+\frac{P_{c1}}{2}\right)\boldsymbol{K}^{-1}\boldsymbol{S} & -\frac{P_{s1}}{2}\boldsymbol{K}^{-1}\boldsymbol{S} \\ -\frac{P_{s1}}{2}\boldsymbol{K}^{-1}\boldsymbol{S} & \boldsymbol{I}-\frac{\theta^2}{4}\boldsymbol{K}^{-1}\boldsymbol{M}-\left(P_0+\frac{P_{c1}}{2}\right)\boldsymbol{K}^{-1}\boldsymbol{S} \end{vmatrix}=\boldsymbol{0}. \tag{22}$$

In this determinant the unknown parameter θ occurs only in the diagonal elements. We can therefore rewrite Eq.(22) as

$$|\boldsymbol{A}-\theta^2\boldsymbol{B}|=\boldsymbol{0}, \tag{23}$$

where the matrices $\boldsymbol{A}$ and $\boldsymbol{B}$ are given by

$$\boldsymbol{A}=\begin{bmatrix} \boldsymbol{I}-\left(P_0+\frac{P_{c1}}{2}\right)\boldsymbol{K}^{-1}\boldsymbol{S} & -\frac{P_{s1}}{2}\boldsymbol{K}^{-1}\boldsymbol{S} \\ -\frac{P_{s1}}{2}\boldsymbol{K}^{-1}\boldsymbol{S} & \boldsymbol{I}-\left(P_0+\frac{P_{c1}}{2}\right)\boldsymbol{K}^{-1}\boldsymbol{S} \end{bmatrix},$$

$$\boldsymbol{B}=\frac{1}{4}\boldsymbol{K}^{-1}\boldsymbol{M}\begin{bmatrix} \boldsymbol{I} & \boldsymbol{0} \\ \boldsymbol{0} & \boldsymbol{I} \end{bmatrix}.$$

We may use methods such as the Jacobi's or Householder method to determine the eigenvalues θ^2 and the corresponding eigenvectors (Bathe, 1998; Antia, 1995) as both the above matrices $\boldsymbol{A}$ and $\boldsymbol{B}$ are symmetric.

Damped case

This is the more general case as almost all structures have some kind of energy dissipation mechanism embedded in them. In this case, all the partitioned matrix sub-elements of Eq.(21) contain the unknown parameter θ and so this problem is more difficult to solve than the previous case.

By equating the determinant of the matrix shown in Eq.(21) to zero, we will get a fourth order equation in terms of θ. This can be written as

$$f(\theta)=0.$$

This is a transcendental equation and can be solved numerically using, for example, the secant method (Antia, 1995; Chapra and Canale, 2000). The secant method is an iterative method used to determine the roots of an equation starting with a pair of assumed values θ_0 and θ_1. At the ith iteration θ_{i+1} is obtained from θ_i and θ_{i-1} as

$$\theta_{i+1}=\theta_i-\frac{(\theta_{i+1}-\theta_i)f(\theta_i)}{f(\theta_{i-1})-f(\theta_i)}.$$

The secant method is a bracketing method and a check is needed at every iteration to ensure that the root always lies within the two selected points θ_i and θ_{i-1}.

Similar considerations hold for solutions of Eq.(6) with period T. Here, we seek a periodic solution with period T in the form

$$q(t)=b_0+\sum_{k=2,4,6,\ldots}^{\infty}\left(a_k\sin\frac{k\theta t}{2}+b_k\cos\frac{k\theta t}{2}\right). \tag{24}$$

Substituting the series Eq.(24) into Eq.(6) and equating the coefficients of identical $\sin(k\theta t/2)$ and $\cos(k\theta t/2)$ terms yields a system of linear homogeneous algebraic equations which can be written in the pattern

sine coefficients at $(2n)$th region (at $k=2n$),

…,

sine coefficients at fourth region (at k=4),
sine coefficients at second region (at k=2),
constant terms at zero region (at k=0),
cosine coefficients at second region (at k=2),
cosine coefficients at fourth region (at k=4),
…,
cosine coefficients at ($2n$)th region (at k=$2n$), which can be written in matrix form as

$$\begin{bmatrix} \cdots & \cdots & \cdots & \cdots & \cdots & \cdots \\ \cdots & e_{11} & e_{12} & e_{13} & e_{14} & \cdots \\ \cdots & e_{21} & e_{22} & e_{23} & e_{24} & \cdots \\ \cdots & e_{31} & e_{32} & e_{33} & e_{34} & \cdots \\ \cdots & e_{41} & e_{42} & e_{43} & e_{44} & \cdots \\ \cdots & \cdots & \cdots & \cdots & \cdots & \cdots \end{bmatrix} \begin{Bmatrix} \cdots \\ a_2 \\ b_0 \\ b_2 \\ b_4 \\ \cdots \end{Bmatrix} = \mathbf{0}. \quad (25)$$

The assumed periodic solution with period T in Eq.(24) gives rise to only even number of regions. For second region we have to consider both sine and cosine coefficients with k=0 and k=2. Likewise we have to consider for higher regions also.

Eq.(25) is a system of homogeneous linear algebraic equations. The condition for existence of nontrivial solutions is that the determinant of the coefficient matrix be equal to zero. Let us first consider the second region alone, which leads to

$$\begin{vmatrix} \boldsymbol{I}-\theta^2\boldsymbol{K}^{-1}\boldsymbol{M}-\left(P_0+\frac{P_{s2}}{2}\right)\boldsymbol{K}^{-1}\boldsymbol{S} & -\left(\frac{P_{s1}+P_{s2}}{2}\right)\boldsymbol{K}^{-1}\boldsymbol{S} & -2\xi\theta\boldsymbol{K}^{-1}\boldsymbol{M}-\frac{P_{s2}}{2}\boldsymbol{K}^{-1}\boldsymbol{S} \\ -\frac{P_{s1}}{2}\boldsymbol{K}^{-1}\boldsymbol{S} & \boldsymbol{I}-P_0\boldsymbol{K}^{-1}\boldsymbol{S} & -\frac{P_{c1}}{2}\boldsymbol{K}^{-1}\boldsymbol{S} \\ -2\xi\theta\boldsymbol{K}^{-1}\boldsymbol{M}-\frac{P_{s2}}{2}\boldsymbol{K}^{-1}\boldsymbol{S} & -\frac{P_{c1}+P_{c2}}{2}\boldsymbol{K}^{-1}\boldsymbol{S} & \boldsymbol{I}-\theta^2\boldsymbol{K}^{-1}\boldsymbol{M}-\left(P_0+\frac{P_{c2}}{2}\right)\boldsymbol{K}^{-1}\boldsymbol{S} \end{vmatrix} = \mathbf{0}. \quad (26)$$

Equating the determinant in Eq.(26) to zero, we obtain an equation for the boundary frequencies. This equation makes it possible to calculate the boundaries of the regions of instability.

The procedure for getting the solution of Eq.(26) is precisely the same as what we have seen while calculating the first region solution. If we need to find the third region then we should go for the periodic solution with period $2T$ [Eq.(19)]. Similarly for the fourth region we should use the periodic solution with period T [Eq.(24)]. Likewise we have to go for higher regions. However, the first region is the most critical among all the others. This region as a result is known as the principal region (Bolotin, 1964).

NUMERICAL RESULTS AND DISCUSSION

A number of numerical examples involving slender columns subjected to periodic axial load with various end-conditions are considered. The stability regions are obtained using the computer codes developed. Newmark's method of direct integration of the equations of motion is used to verify the results in each case. The programs have been developed based on Object Oriented Programming (OOP) concepts and use several objects including matrix and vector classes. Comparison of the results with analytical/computational results available in the literature was also carried out. A total of six problems are considered.

Example 1: Undamped vibration of hinged-hinged column under harmonic load

A hinged-hinged column subjected to a harmonic axial load $P_d\cos\theta t$ as shown in Fig.4a is considered. The data used for all the problems discussed in this paper are: l=7 m; E=2.1×10^{11} MPa; J=2.003×10^{-5} m^4.

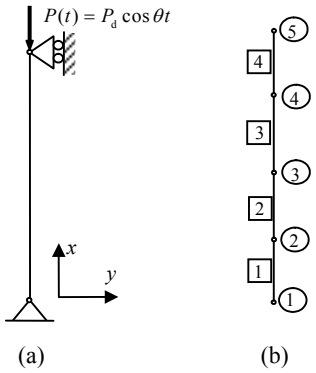

Fig.4 Hinged column subjected to periodic (a) and its finite element discretisation (b)

The column has been discretised into four equal-sized beam elements as depicted in Fig.4b. The element and node numbers are also indicated in the figure. At each node there is a transverse displacement degree of freedom and a rotation.

Instability region of this case along with analytical results (Bolotin, 1964) is shown in Fig.5. It can

be seen that the finite element solution is slightly shifted from the exact solutions. This can lead to an overestimation of buckling load for a given frequency of loading. A finer discretisation of the problem using elements of smaller size leads to closer results. A four-element discretisation was found to be reasonably good. A direct integration using Newmark's method is carried out to verify the reliability of the above procedure. The following parameters (Bathe, 1998) are employed: δ=0.5, α=0.25 and $\Delta t=5\times10^{-4}$ s. An initial transverse displacement of 30 mm is imposed corresponding to the translation degree of freedom at node 3.

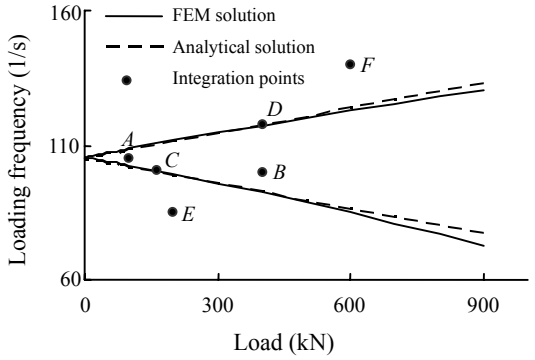

Fig.5 Instability region obtained using finite element method and analytical solution

Six points indicated as *A* to *F* in Fig.5 are considered. The coordinates of these points are given in Table 1. The column subjected to harmonic loading is analysed using Newmark's method. The transverse displacements of node 3 (i.e., the mid-point of the column) are plotted with respect to time for each of these cases and are shown in Figs.6a to 6f.

Figs.6a and 6b clearly indicate instability, the amplitude increasing more rapidly in the latter case. Figs.6d and 6d show periodic oscillation along with the so-called beat phenomenon. In Figs.6e and 6f two cases of stability in which the displacement is limited are shown.

Example 2: Damped vibration of hinged-hinged column under harmonic load

The consideration of damping of the system

Table 1 Coordinates of salient points in Fig.5

Integration point	Coordinate	
	θ (s^{-1})	P_d (kN)
A	105.52	100
B	100.00	400
C	100.85	160
D	117.70	400
E	85.00	200
F	140.00	600

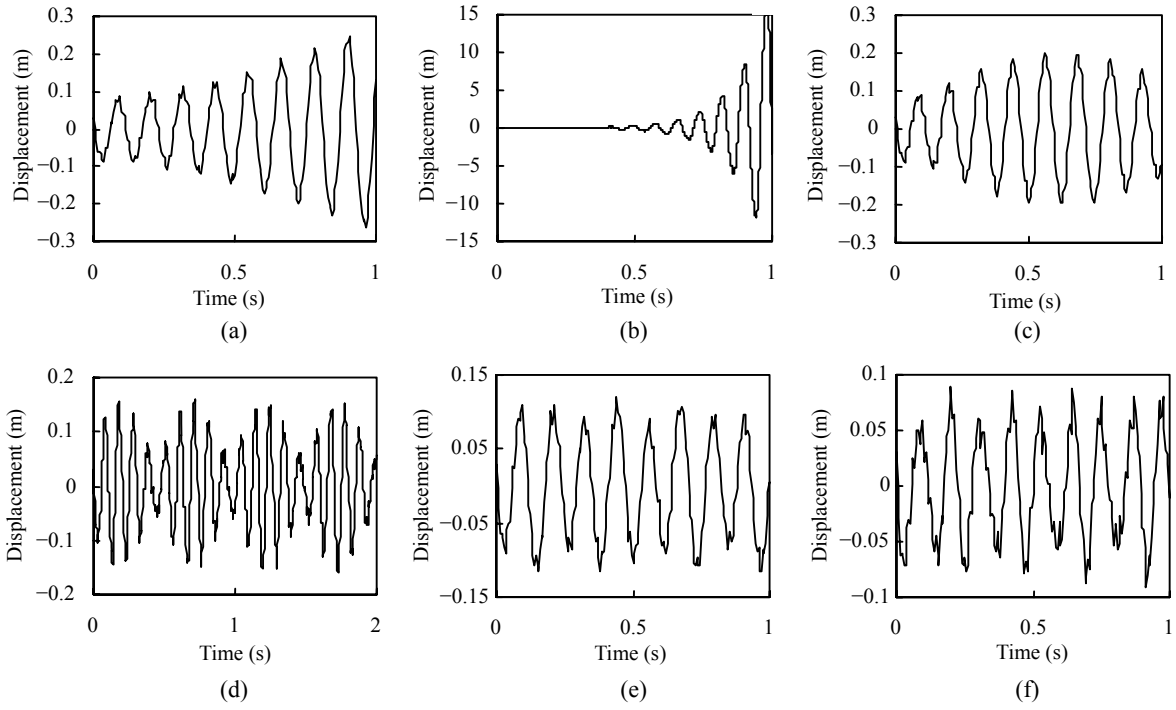

Fig.6 Displacement versus time diagram for integration points *A* (a) to *F* (f) of Fig.5

improves the stability in most of the cases. The hinged-hinged column shown in Fig.4a with the proportional damping factor of α=5 s^{-1} is considered as the next example.

The principal region of instability is shown in Fig.7 for this case. The analytical solution for the undamped case is also indicated in the figure. To check the correctness of the results, the Newmark's direct integration method is used. Five points indicated *A* to *E* in Fig.7, whose coordinates are given in Table 2, are considered. The transverse displacements of node 3 are plotted with respect to time for these cases and are shown in Figs.8a to 8e.

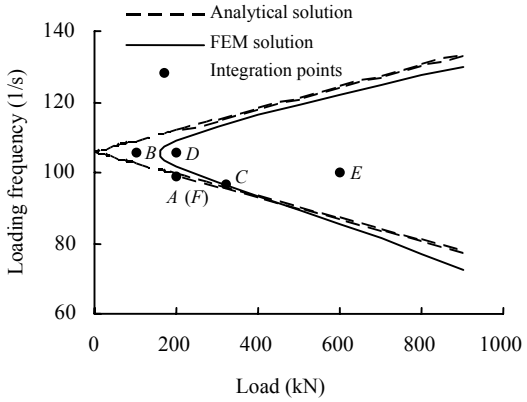

Fig.7 Instability region obtained using finite element method and analytical solution for the damped case

Figs.8a and 8b are characterised by a displacement function whose amplitude decreases exponentially with time finally reaching a zero value denoting asymptotic stability. In Fig.8c the solution is periodic and lies on the boundary between stability and instability regions. Fig.8d and 8e indicate exponentially increasing amplitude of vibration denoting instability.

The first two regions of instability corresponding to the lowest frequency of vibration of the column of Fig.4a are shown in Fig.9. Higher regions of instability are smaller in size, and their significance further decreases in the presence of damping. The results of numerical integrations at the points reported in Table 3 are shown in Figs.10a to 10c; previous results are again confirmed.

Table 2 Coordinates of the integration points indicated in Fig.7

Integration point	Coordinate	
	θ (s^{-1})	P_d (kN)
A	100.00	200
B	105.52	100
C	96.73	320
D	105.52	200
E	100.00	600
F	100.00	200

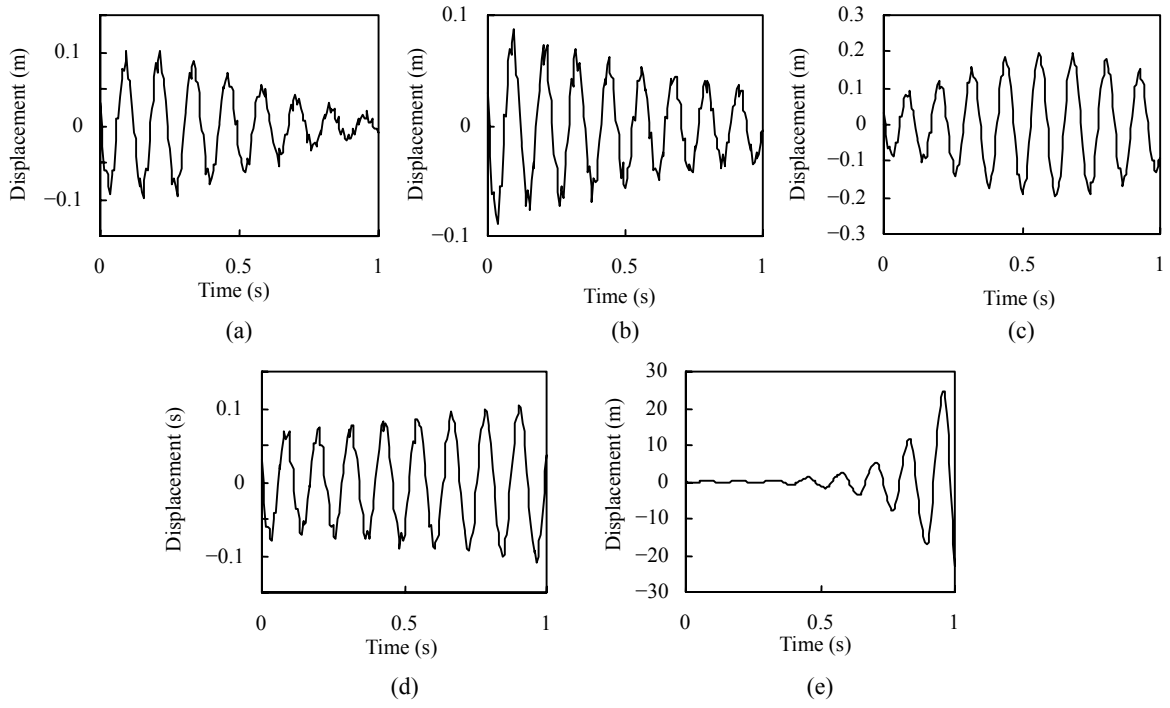

Fig.8 Displacement versus time diagram for integration points *A* (a) to *E* (e) of Fig.7

Table 3 Coordinates of points for the second region in the presence of damping, see in Fig.8

Integration point	Coordinate	
	θ (s^{-1})	P_d (kN)
A	51	600
B	54	700
C	50	800

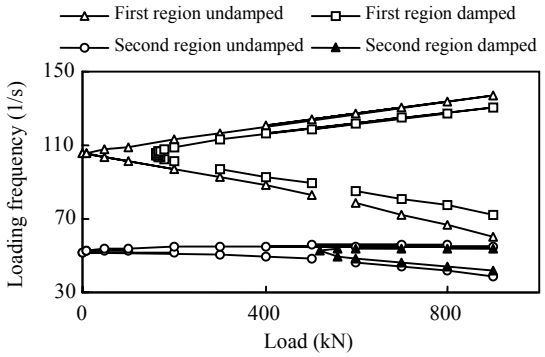

Fig.9 The first two regions of instability of the beam of Fig.2 in the presence of damping

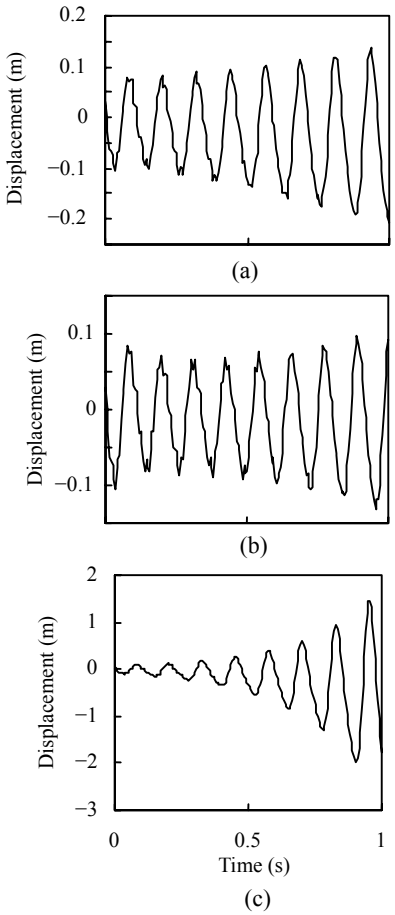

Fig.10 Displacement versus time diagram for integration points *A* (a) to *C* (c) in Table 3

Example 3: Undamped vibration of hinged-hinged column under periodic load

A hinged-hinged column subjected to a periodic axial load is considered. The loading is given by $F(t)=(F_0/T)t$, $0\le t\le T$ as depicted in Fig.11. The first two terms of the periodic loading are $P(t)=F_0/2-F_0\times\sin[(\theta/\pi)t]$.

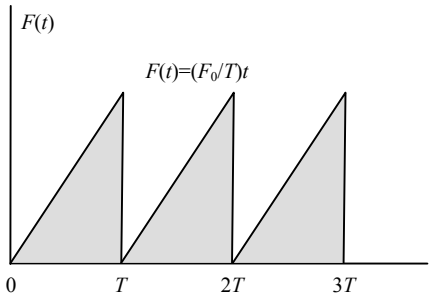

Fig.11 Periodic load

The principal regions of instability are shown in Fig.12. A direct integration using Newmark's method is carried out corresponding to six points indicated *A* to *F* in Fig.12. The coordinates of these points are given in Table 4. The transverse displacements of node 3 (i.e., the mid-point) are plotted with respect to time for each of these cases and are shown in Figs.13a to 13f. While Figs.13a and 13b indicate instability, Figs.13e to 13f indicate stable behaviour; Fig.13c depicts the border case of periodic solution.

Example 4: Damped vibration of hinged-hinged column under periodic load

Taking the same load in Example 4, the principal region of instability is shown in Fig.14. Coordinates of direct integration points indicated by *A* to *E* in Fig.14 are considered and are given in Table 5. The transverse displacements of node 3 are plotted with respect to time for each of these cases and are shown in Figs.15a to 15e. Figs.15a and 15b show stable behaviour, Fig.15c shows periodic solution and Figs.15d and 15e depict unstable behaviour.

CONCLUSION

The FEM using simple beam elements is shown to be very useful in dealing with dynamic stability problems of columns and frames. Although the

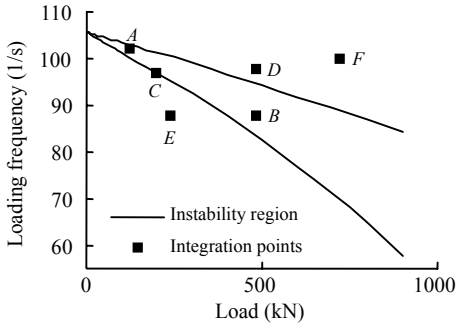

Fig.12 Principal regions of instability of the column under periodic loading

Table 4 Coordinates of points *A* to *F* of Fig.12

Integration point	Coordinate	
	θ (s^{-1})	P_d (kN)
A	102	120
B	88	480
C	97	200
D	98	480
E	88	240
F	100	720

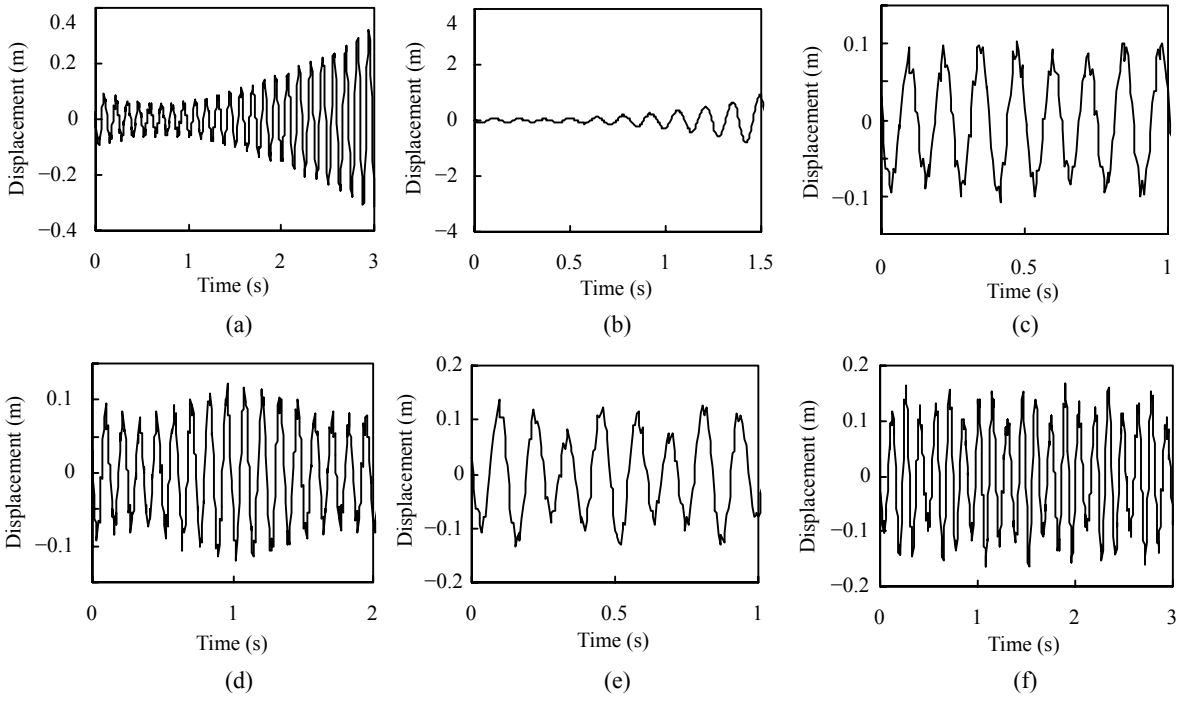

Fig.13 Displacement versus time diagram for integration points *A* (a) to *F* (f) of Fig.12

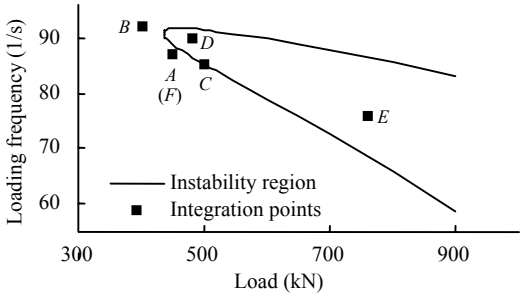

Fig.14 Principal regions of instability in presence of damping

Table 5 Coordinates of points *A* to *F* of Fig.14

Integration point	Coordinate	
	θ (s^{-1})	P_d (kN)
A	87	450
B	92	400
C	85	500
D	90	480
E	76	760
F	87	450

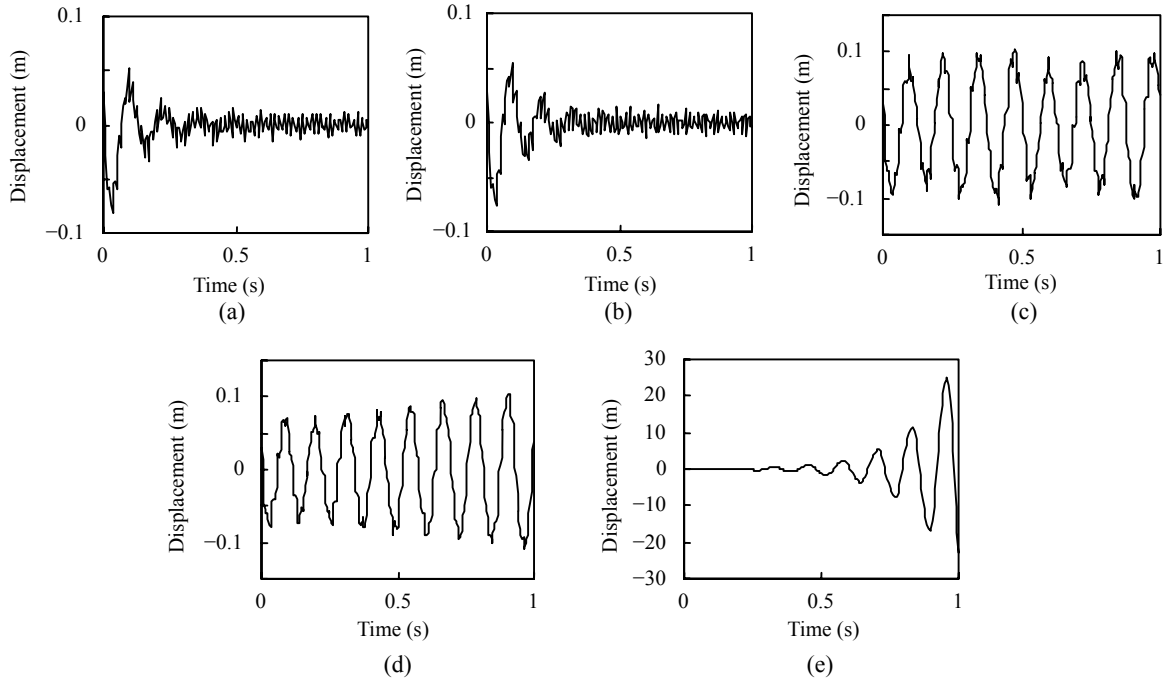

Fig.15 Displacement versus time diagram for integration points *A* (a) to *E* (e) of Fig.14

examples presented in this paper do not include frames the proposed method is applicable for the analysis of frames as well. For a given loading frequency, FEM slightly over-estimates the buckling load when compared to the exact solution using a continuum model. In the presence of damping, the loss of dynamic stability of the straight form of rod can occur only at the amplitude of the longitudinal force greater than a certain minimum value. To verify the reliability of the above procedure direct integration using Newmark's method is considered. It is used to check the instability regions by plotting the displacement vs time diagram of a particular direct integration point, which shows the loading frequency and loading amplitude in the instability regions. A coordinate of direct integration in the instability region shows an exponentially increasing oscillation with time and one in the stability region shows that the vibration of the rod is decaying with time, and one on the boundary region shows the periodic vibration with time.

References

Antia, H.M., 1995. Numerical Methods for Scientists and Engineers. Tata McGraw Hill, New Delhi.

Bathe, K.J., 1998. Finite Element Procedures. Prentice-Hall, Englewood Cliffs.

Bolotin, V.V., 1964. The Dynamic Stability of Elastic Systems. Holden Day, San Francisco.

Briseghella, L., Majorana, C.E., Pellegrino, C., 1998. Dynamic stability of elastic structures: A finite element approach. *Computers & Structures*, **69**(1):11-24. [doi:10.1016/S0045-7949(98)00084-4]

Chapra, S.C., Canale, P.R., 2000. Numerical Methods for Engineers. Tata McGraw Hill, New Delhi.

Cook, R.D., Malkus, D.S., Plesha, M.E., Witt, R.J., 2003. Concepts and Applications of Finite Element Analysis. John Wiley & Sons, New York.

Javidruzi, M., Vafai, A., Chen, J.F., Chilton, J.C., 2004. Vibration, buckling and dynamic stability of cracked cylindrical shells. *Thin-Walled Structures*, **42**(1):79-99. [doi:10.1016/S0263-8231(03)00125-3]

McLachlan, N.W., 1957. Theory and Applications of Mathieu Functions. Oxford University Press, New York.

Meirovitch, L., 1970. Methods of Analytical Dynamics. McGraw Hill, New York.

Park, H.I., Jung, D.H., 2002. A finite element method for dynamic analysis of long slender marine structures under combined parametric and forcing excitations. *Ocean Engineering*, **29**(11):1313-1325. [doi:10.1016/S0029-8018(01)00084-1]

Sugiyama, Y., Katayama, K., Kiriyama, K., 2000. Experimental verification of dynamic stability of vertical cantilevered columns subjected to a sub-tangential force. *Journal of Sound & Vibration*, **236**(2):193-207. [doi:10.1006/jsvi.1999.2969]

Sygulski, R., 1996. Dynamic stability of pneumatic structures in wind: theory and experiment. *Journal of Fluids & Structures*, **10**(8):945-963. [doi:10.1006/jfls.1996.0060]

Zounes, R.S., Rand, R.H., 1998. Transition curves for the quasi-periodic Mathieu Equation. *SIAM J. Appl. Math.*, **58**(4):1094-1115. [doi:10.1137/S0036139996303877]